Int J Clin Exp Med 2021;14(2):915-923
www.ijcem.com /ISSN:1940-5901/IJCEM0122549

Original Article

Assessing the effects of miR-145 on the radiosensitivity of breast cancer cells and the underlying molecular mechanism

Caijie Liao[1*], Lingling Ye[2*]

[1]*The First Clinical Medical School, Guangzhou University of Chinese Medicine, Guangzhou, Guangdong Province, China;* [2]*Galactophore Department of The Second Affiliated Hospital, Guangzhou University of Chinese Medicine, Guangzhou, Guangdong Province, China.* [*]*Equal contributors and co-first authors.*

Received September 16, 2020; Accepted October 14, 2020; Epub February 15, 2021; Published February 28, 2021

Abstract: Purpose: To explore the contribution of miR-145 to the radiosensitivity of MDA-MB-231 cells and to understand the molecular mechanism. Methods: MDA-MB-231 cells were divided into a blank control group (BCG), a negative control group (NCG), and a miR-145-mimics group. qPCR was used to measure the expression of miR-145 and OCT4 mRNA at 48 h after transfection. A colony formation assay was used to determine the radiosensitivity of the transformed cells. Western blot analysis was conducted to assess OCT4, E-cadherin, and vimentin protein levels. MTT assay and flow cytometry were performed to evaluate proliferation and apoptosis, respectively, whereas a luciferase reporter assay was used to establish a correlation between miR-145 and OCT4. Results: miR-145 expression was downregulated in the MDA-MB-231 cells ($P < 0.05$), whereas miR-145 expression levels increased after transfection ($P < 0.05$). The miR-145-mimics group exhibited lower survival fraction, OCT4 mRNA and protein levels, vimentin levels, cell proliferation rate and higher E-cadherin protein levels and apoptosis than the other two groups ($P < 0.05$). The miR-145-mimics group exhibited lower luciferase activity with the 3 UTR gene vector of wild-type OCT4 than the NCG ($P < 0.05$). Group A exhibited lower OCT4 mRNA and protein levels and E-cadherin protein levels and higher vimentin levels and apoptosis than group B ($P < 0.05$). Conclusion: MiR-145 expression levels in breast cancer cells (BCCs) decreased. Overexpression of miR-145 induces epithelial–mesenchymal transition in BCCs, regulates cell proliferation and relocation, and increases radiosensitivity. These processes may be related to specific binding sites within the 3 UTR of OCT4.

Keywords: Breast cancer, miR-145, radiosensitivity, molecular mechanism

Introduction

Breast cancer accounts for 8%-12% of all malignancies, and the 5-year survival rate is 62.4% [1, 2]. Local radiotherapy is currently one treatment option, and it can greatly reduce the recurrence rate and the mortality rate of patients with breast cancer. However, radiation resistance remains a challenging obstacle to the overall effectiveness of radiation therapy [3-5].

MicroRNA (miRNA) represents a series of endogenous noncoding RNAs that can inhibit gene expression or translation by binding to a complementary sequence in the 3 untranslated region (3 UTR) of its target gene [6, 7]. Some studies have shown that miRNAs exhibit a direct correlation with tumor occurrence and that they may affect radiation resistance. Therefore, exploiting miRNAs to attenuate gene expression offers a novel strategy to increase radiosensitization [8-10]. The miRNA, miR-145, is localized on chromosome 5q32-33. The miR-145 expression level in tumor tissue is significantly decreased, whereas its overexpression suppresses tumor cell growth and dramatically decreases cell migration. Studies have shown that miR-145 may also effectively increase tumor sensitivity to chemotherapy drugs. In addition, miR-145 is a useful biomarker for colorectal, pancreatic, and breast cancers [11-13].

In a study by Ye et al. [14], miR-145 expression inhibited breast cancer cell (BCC) proliferation, colony formation, migration, and invasion. MiR-145 partially represses the proliferation of lung cancer initiating cells and epithelial-mesenchymal transition (EMT) by regulating the octamer-binding transcription factor 4 (OCT4) expression, thereby inhibiting tumor growth and metastasis [15]. EMT is a signaling pathway associated with tumor cell metastasis that influences migration and invasion [16]. At the early stages of the differentiation process, EMT relies on the expression of epithelial cadherin (E-cadherin), N-cadherin, and vimentin, as evidenced by E-cadherin downregulation and elevated vimentin and N-cadherin expression [17]. However, there are no studies describing a role of miR-145 in BCC radiosensitivity and the underlying molecular mechanism responsible for its effect.

Materials and methods

Cell sourcing

The human BCC line, MDA-MB-231 (No. BNCC337893); the normal human breast cell line, Hs 578Bst (No. BNCC3376680); and the human embryonic kidney cell line, HEK-293 (No. BNCC338274) were purchased from Beiner Bio. The cells were cultured in DMEM (Shanghai Junrui Biotechnology Co., Ltd., No. UFP0590) plus 10% fetal bovine serum (Bovogen Biological company, No.C0230), 100 U/ml penicillin (Biyuntian Biotechnology Co., Ltd.), and 100 μg/ml streptomycin (Biyuntian Biotechnology Co., Ltd.) at 37°C in 5% CO_2 in a humidified incubator.

Cell processing

MDA-MB-231 and Hs 578Bst cells were plated and when the adherent growth density reached 90% confluence, the cells were digested with 0.25% trypsin. Once the cells became round and started to detach, DMEM medium was added, and the cells were re-cultivated at 37°C in a 5% CO_2 atmosphere. Cells from the third generation of culture were collected.

MDA-MB-231 breast cancer cells were divided into a blank control group (BCG) that was not infected with lentivirus, a negative control group (NCG) that was infected with a negative control lentivirus, and an miR-145-mimics group, which was infected with lentivirus packaged with an miR-145 overexpressing construct. The following assays were simultaneously performed on the three cell groups.

Transfection and construction

The miR-145 expression vector (miR-145-mimics group) and its corresponding unrelated control sequences (NCG) and miR blank vector (BCG) were designed and synthesized by Thermo Fisher Scientific. MDA-MB-231 cells were trypsinized for 1 day before transfection, and the expression vector was transfected when the cells reached 80% confluence. Afterwards, the cells were cultivated at 37°C in 5% CO_2 for 2 days, and the medium was changed every 6 h. The Lipofectamine TM 2000 transfection kit was provided by Beijing Solibao Technology Co., Ltd (11668-027) and used according to the manufacturer's instructions.

qPCR

Total RNA was extracted from serum and cultured cells using a Trizol extraction kit (Invitrogen, Carlsbed, CA, USA). A Nano-Drop2000 UV spectrophotometer (Beijing Keyu Xingye Technology Development Co., Ltd., China) was used for determining RNA concentration and purity. RNA was reverse-transcribed to cDNA using a reverse transcription kit (Invitrogen, Carlsbed, CA, USA), and the resulting cDNA was stored at -20°C. PCR primers were designed and prepared by Shanghai Jima Pharmaceutical Technology Co., Ltd.; PCR was conducted using a PCR instrument (Applied Biosystems, Foster City, CA, USA) using the following program: 90°C for 5 min, 90°C for 5s, 60°C for 30s, 72°C for 5s over 40 cycles. Each sample was analyzed three times, and the relative expression of each gene was calculated using the $2^{-\Delta\Delta CT}$ method.

Detection of protein expression using western blot (WB) analysis

Total protein was isolated using RIPA lysis buffer, and its concentration was determined by the BCA assay. Protein concentrations were adjusted to 4 μg/μL and separated on 12% SDS-PAGE gels with a voltage ranging from 90 to 120 V. Following electrophoresis, proteins were transferred to PVDF membranes at 100 V for 100 min. The membranes were blocked with 5% skim milk for 1 h at 37°C, followed by an overnight incubation with primary antibody (1:1000) at 4°C. After washing three times with

PBS, the membranes were incubated with secondary antibody (1:1000) for 60 min at room temperature. The membranes were developed using an ECL luminescence kit and quantified with Quantity One. Relative protein expression = band gray value/internal control gray value. The RIPA kit (#89901), BCA protein kit (#232-50), ECL luminescence kit (#35055), and protease (#90058) were purchased from Thermo Fisher Scientific. Rabbit anti-OCT4 protein (ab38594), anti-E-cadherin (ab56326), vimentin monoclonal antibody (ab35637), and goat anti-rabbit IgG secondary antibody (ab6721) were obtained from Abcam.

Cell irradiation

Cells were irradiated with 0.363 $Gy \cdot min^{-1}$, at 60-cm target-skin distance using a Philips X-ray therapy machine (180 kV, 18 mA). The absorbed doses were delivered as single doses at 0, 1.0, 2.0, 3.0, 4.0, and 6.0 Gy.

Cell cloning

The irradiated cells were continuously cultured in an incubator for 15 days. The cells were then rinsed twice with PBS buffer, fixed with anhydrous MeOH, and stained with Giemsa dye. Cell colonies containing over 50 cells were counted through a microscope, and the clone generation rate (CGR), equal to the number of clones generated/number of seeded cells × 100%, was determined. The survival fraction (SF) was also calculated (SF = CGR of irradiated cells/CGR of control group × 100%).

Detection of cell proliferation

Next, 24 h after transfection, MDA-MB-231 cells were seeded into 96-well plates (1×10^4 cells per well) and incubated at 37°C for 48 h. Subsequently, 20 μL of MTT solution (5 μg/mL) was added. Following a 4-h incubation at 37°C, the absorbance (490 nm) for each well was measured. The MTT detection kit was obtained from Beijing Equation Jiahong Technology Co., Ltd.

Apoptosis detection

Flow cytometry (FC) was used to assess apoptosis. Following transfection, MDA-MB-231 cells were digested with trypsin (0.25%), rinsed with PBS twice, and mixed with 100 μL of binding buffer to obtain a suspension of 1×10^6 cells/mL. Cells were incubated with AnnexinV-FITC/PI staining reagent at room temperature and protected from light for 15 min according to the manufacturer's instructions (Biyuntian Biotechnology Research Institute). The apoptosis rate was detected using the FC500MCL flow cytometer system, and the average value of three measurements was recorded.

Luciferase reporter assay

The 3 UTR sequence of wild-type OCT4 and mutations in the 3'UTR sequence were inserted into the *XhoI/NotI* site of the psicheck2 vector to construct a luciferase reporter plasmid. HEK293T cells were cultured to 70% confluency. Lipofectamine 2000 was used to transfect psicheck2-OCT4 3 UTR and its mutant plasmids, 100 nmol/L miR-145 mimics (miR-145-mimics) or random sequences (NC group) into HEK293T cells. The relative luciferase activity was measured after 48 h.

Effect of miR-145 on OCT4 expression

The miR-145 and OCT4 mRNA overexpression vectors were designed and synthesized by Thermo Fisher Scientific for co-transfection into MDA-MB-231 cells. These were classified as group A (miR-145-mimics) and group B (miR-145-mimics + OCT4 mRNA overexpression). Next, 48 h after transfection, qPCR and WB analysis were used for determining the levels of OCT4 mRNA and OCT4 protein, respectively, in both groups in addition to E-cadherin and vimentin protein expression. MTT assay was used to detect proliferation. FC was used to detect apoptosis and the effects on radiosensitivity were determined.

Statistical methods

SPSS 20.0 (SPSS Co., Ltd. in Chicago, the United States) was used for statistical calculations. GraphPad Prism 7 (Graphpad Software Co., Ltd. in San Diego, the United States) was used for figure illustrations. Count data were presented as rates and compared using the χ^2 test. The measured data were expressed as average ± standard deviation. A *t*-test was conducted for determining differences between two groups and ANOVA for the distinctions between multiple groups. *P*-values < 0.05 were considered statistically significant.

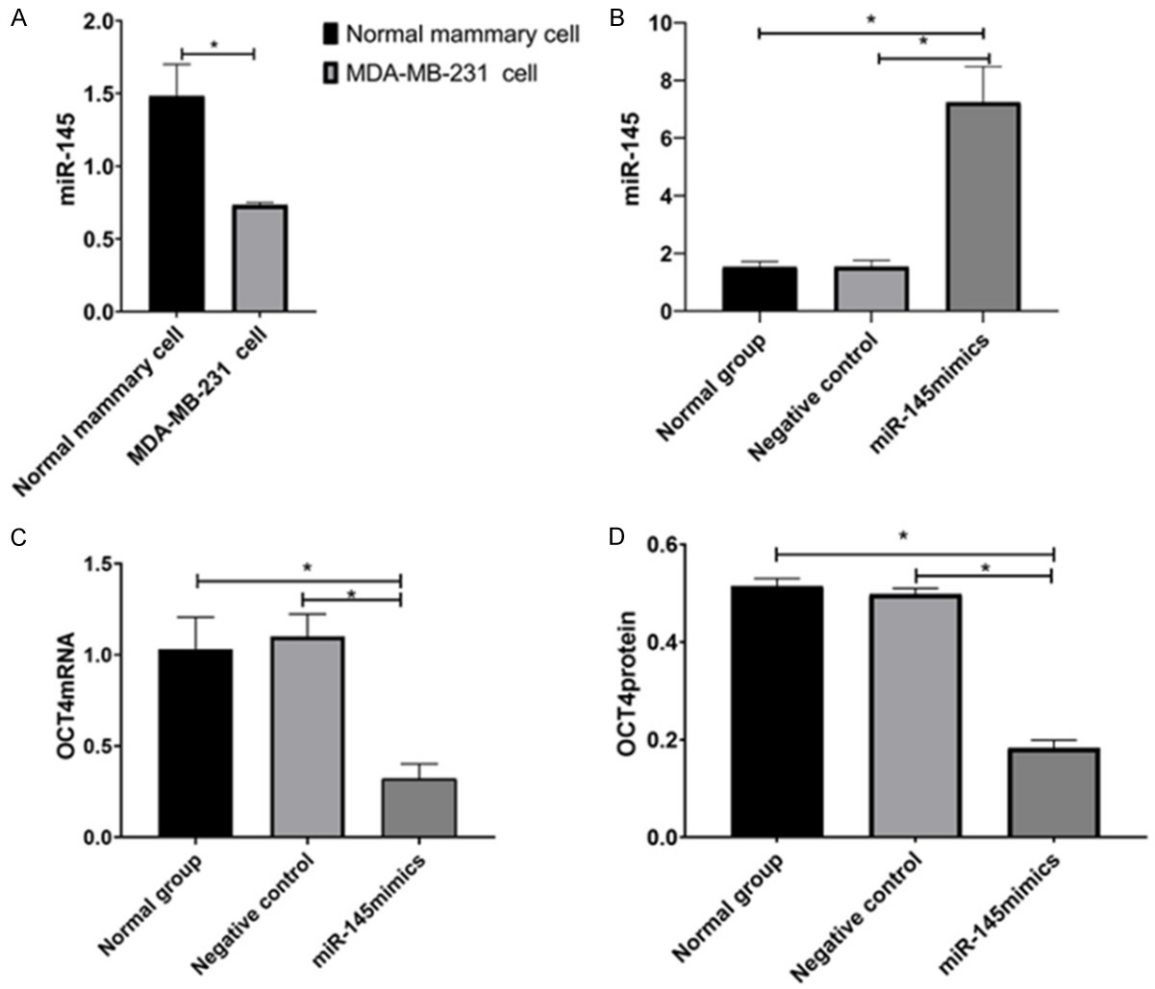

Figure 1. OCT4 mRNA and protein levels in MDA-MB-231 cells after miR-145 overexpression. A. miR-145 expression levels. *P < 0.05 compared with healthy breast cells. B. MDA-MB-231 cell transfection. * compared with miR-145-mimics. P < 0.05. C. OCT4 mRNA level. D. OCT4 protein level. * compared with miR-145-mimics. P < 0.05.

Results

miR-145 expression

The miR-145 expression levels in normal breast cells and MDA-MB-231 cancer cells were 1.482 ± 0.218 and 0.727 ± 0.016, respectively, and exhibited a significant difference (P < 0.05, **Figure 1**).

MDA-MB-231 cell transfection

The miR-145 expression levels in BCG, NCG, and miR-145-mimics group were 1.531 ± 0.189, 1.541 ± 0.218, and 7.242 ± 1.234, respectively. After transfection, the miR-145 expression in the miR-145-mimics group was dramatically higher than that of BCG and NCG (P < 0.05) (**Figure 1**).

Effect of miR-145 overexpression on MDA-MB-231 cell radiosensitivity

The SF of the miR-145-mimics group at 2, 4, and 6 Gy was notably lower than that of BCG and NCG (P < 0.05) (**Table 1**).

Effect of miR-145 overexpression on OCT4 levels in MDA-MB-231 cells

The OCT4 mRNA levels of blank, negative, and miR-145-mimic groups were 1.032 ± 0.174, 1.102 ± 0.121, and 0.321 ± 0.081, respectively, whereas the OCT4 protein levels were 0.515 ± 0.015, 0.498 ± 0.012, and 0.183 ± 0.016, respectively. The miR-145-mimics group showed significantly decreased OCT4 mRNA and protein levels compared with other two groups (P < 0.05) (**Figure 1**).

Table 1. Survival fraction of miR-145 overexpressing cells at different irradiation doses

Doses	Blank	Negative	miR-145-mimics	F	P
0 Gy	1.000	1.000	1.000		
2 Gy	0.511 ± 0.041*	0.591 ± 0.038*	0.251 ± 0.215	5.763	0.040
4 Gy	0.163 ± 0.026*	0.183 ± 0.019*	0.069 ± 0.011	28.800	< 0.001
6 Gy	0.049 ± 0.007*	0.053 ± 0.010*	0.019 ± 0.004	18.840	0.003
8 Gy	0.015 ± 0.003	0.017 ± 0.007	0.012 ± 0.004	0.770	0.504

Note: *compared with miR-145-mimics P < 0.05.

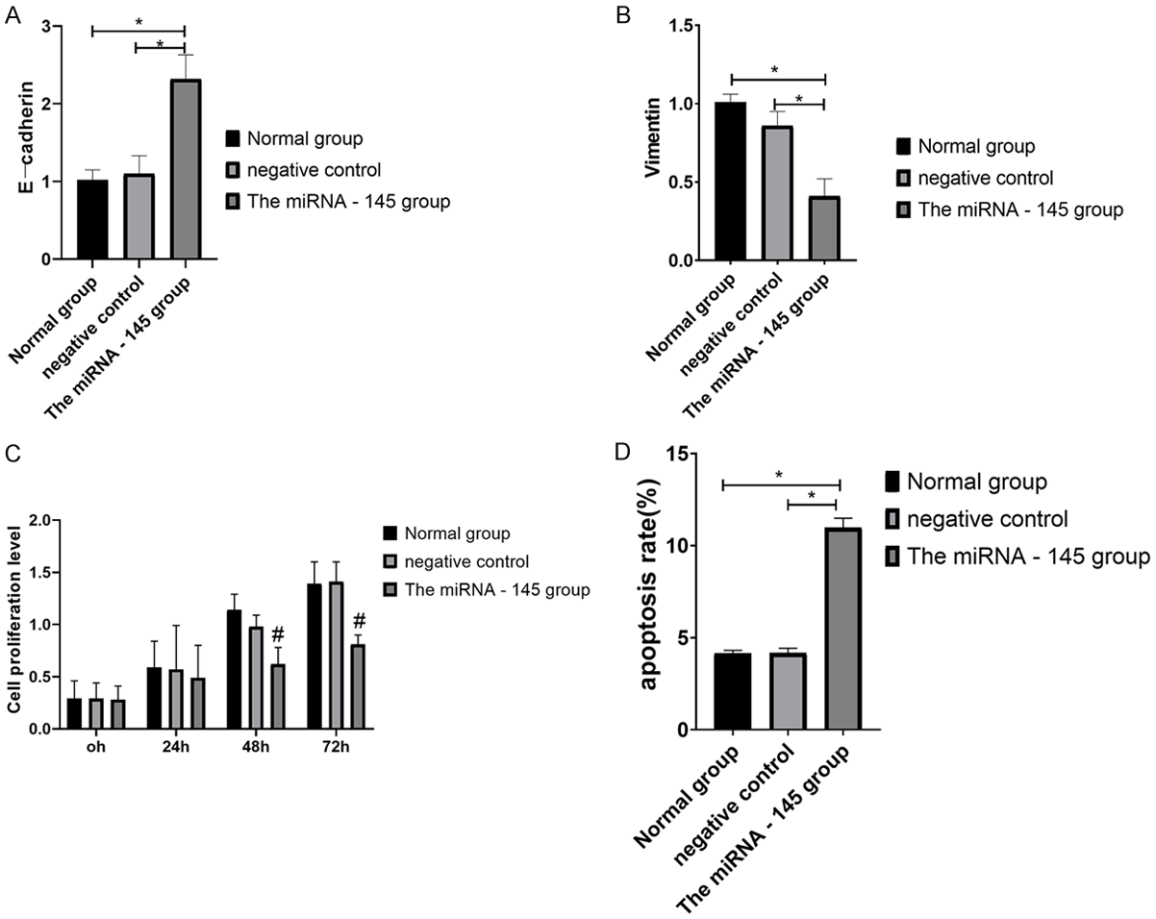

Figure 2. E-cadherin and vimentin protein expression levels and proliferation and apoptosis rates of MDA-MB-231 cells. A. E-cadherin protein expression level. B. Vimentin protein expression level. C. The proliferation level in miR-145-mimics is lower compared with the other two groups. D. Apoptosis rate. *P < 0.05 compared with miR-145-mimics, #P <0.05 compared with the blank control group and negative control group.

E-cadherin and vimentin protein expression levels and proliferation and apoptosis rate in MDA-MB-231 cells

The miR-145-mimics group exhibited higher E-cadherin protein levels and lower vimentin protein levels than the other two groups (P < 0.05). miR-145-mimics group displayed lower proliferation than other two groups at 2 and 3 days (P < 0.05). The apoptosis rate of miR-145-mimics was higher than that of the other two groups (P < 0.05). (**Figure 2**).

Validation of miR-145 targeting of OCT4

The luciferase activity of the wild-type OCT4 3'UTR gene vector in the miR-145-mimics and NC groups was 0.318 ± 0.021 and 1.103 ± 0.017. The luciferase activity of the mutant OCT4 3'UTR gene vector was 1.085 ± 0.009

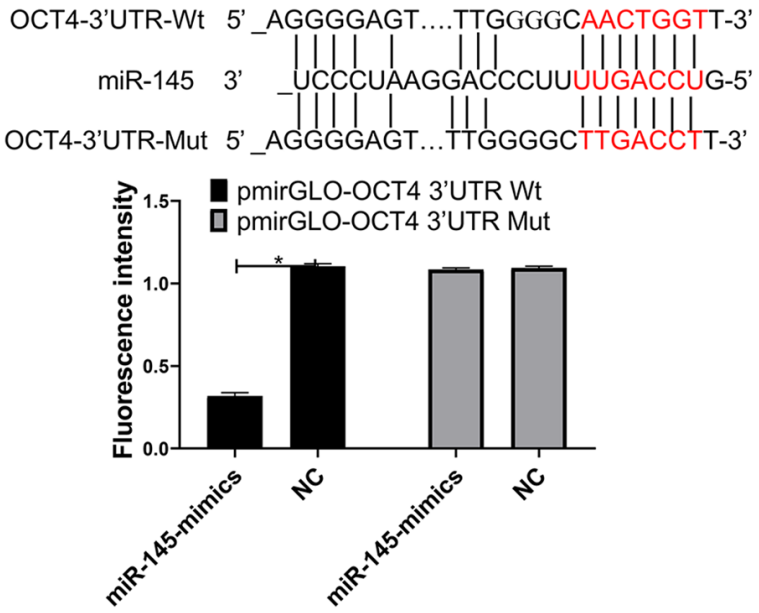

Figure 3. Results of luciferase activity assay. *P < 0.05 compared with NC group.

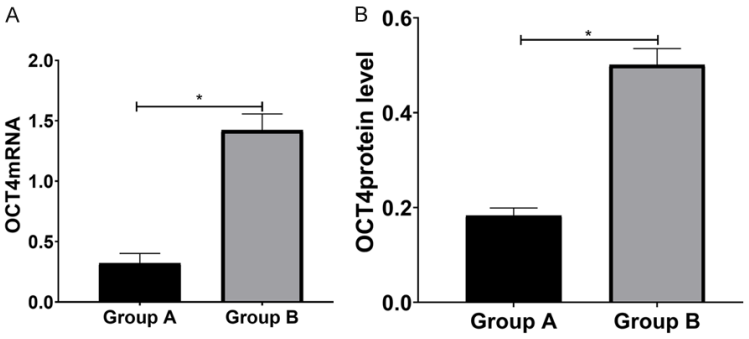

Figure 4. OCT4 mRNA and protein levels in MDA-MB-231 cells after OCT4 overexpression. A. OCT4 mRNA level. B. OCT4 protein level. *P < 0.05 compared with group A. Note: Group A (miR-145-mimics) and group B (miR-145-mimics + OCT4 mRNA overexpression).

Table 2. SF evaluation in two groups

Doses	A	B	F	P
0 Gy	1.000	1.000		
2 Gy	0.251 ± 0.215	0.640 ± 0.091*	2.875	0.045
4 Gy	0.069 ± 0.011	0.173 ± 0.015*	9.684	0.001
6 Gy	0.019 ± 0.004	0.049 ± 0.010*	4.825	0.009
8 Gy	0.012 ± 0.004	0.015 ± 0.006	0.721	0.511

Note: Group A (miR-145-mimics); group B (miR-145-mimics + OCT4 mRNA overexpression). *Compared with miR-145-mimics P < 0.05.

and 1.094 ± 0.011 in the miR-145-mimics and NC groups, respectively. The miR-145-mimics showed a lower luciferase activity than the NC group for the wild-type OCT4 3'UTR gene vector (P < 0.05, **Figure 3**).

Effect of OCT4 overexpression on OCT4 levels in MDA-MB-231 cells

The OCT4 mRNA levels in group A and B were 0.321 ± 0.081 and 1.423 ± 0.134 respectively, whereas the OCT4 protein levels were 0.183 ± 0.016 and 0.501 ± 0.034, respectively. Group A exhibited lower OCT4 mRNA and protein levels than group B (P < 0.05, **Figure 4**).

Effect of OCT4 overexpression on the radiosensitivity of MDA-MB-231 cells

Group A exhibited notably lower SF at 2, 4, 6 Gy than group B (P < 0.05, **Table 2**).

E-cadherin and vimentin protein expression levels and MDA-MB-231 cell proliferation and apoptosis following OCT4 overexpression

The WB results indicated that E-cadherin protein levels in groups A and B were 2.326 ± 0.317 and 1.011 ± 0.018, respectively, whereas the vimentin protein levels in group A and B were 0.41 ± 0.11 and 1.14 ± 0.13 (P < 0.05). Group A displayed higher E-cadherin protein and lower vimentin protein levels than group B (P < 0.05). Group A exhibited a lower cell proliferation rate than group B at 2 and 3 days (P < 0.05), and no difference was found between the two groups at 0 and 1 day (P > 0.05). Group A exhibited a higher apoptosis rate (10.974 ± 0.514%) than group B (3.927 ± 0.219%) (P < 0.05, **Figure 5**).

Discussion

Angiogenesis contributes to the growth, metastasis, and development of tumors. Tumor cells enable endothelial precursor cells to absorb

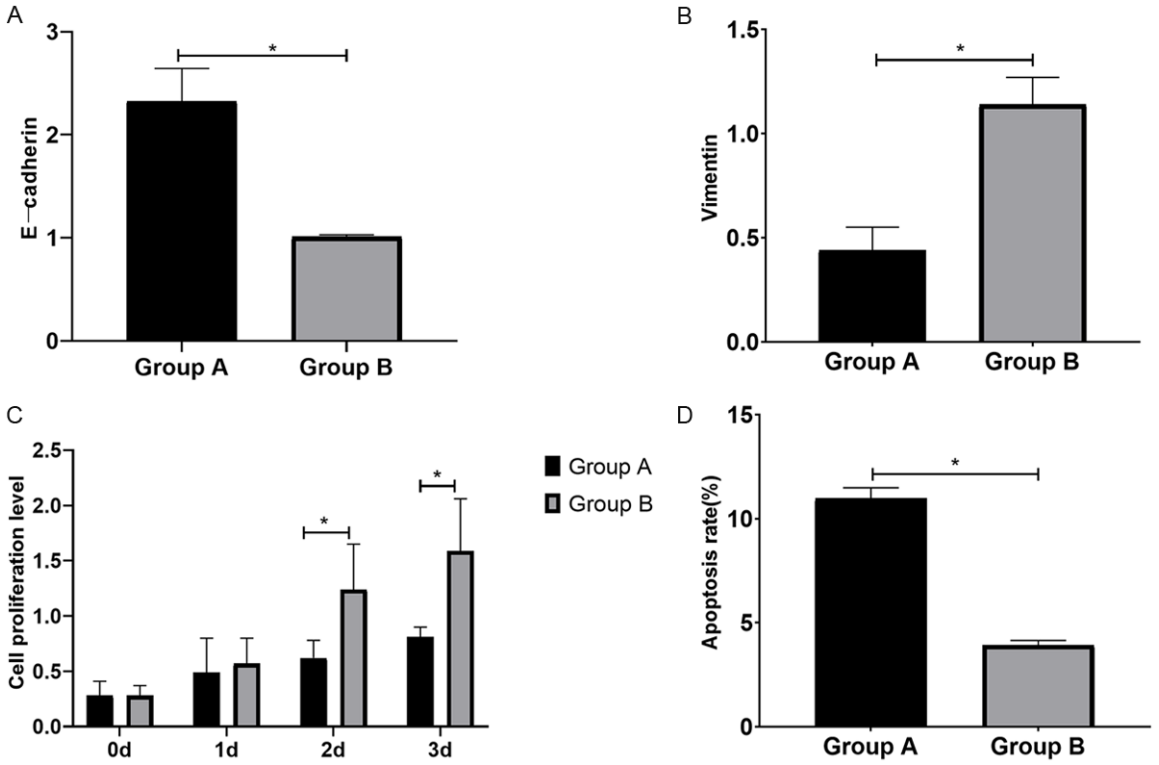

Figure 5. E-cadherin and vimentin protein expression levels and MDA-MB-231 cell proliferation and apoptosis rates after OCT4 overexpression. A. E-cadherin protein expression level. B. Vimentin protein expression level. C. Cell proliferation rate. D. Apoptosis rate. *P < 0.05 compared with group A. Group A (miR-145-mimics) and group B (miR-145-mimics + OCT4 mRNA overexpression).

vascular permeability factors and penetrate the walls of blood vessels. This leads to the transfer of nearby blood vessels toward the core of the tumor, which releases proangiogenic stimuli, thus enabling tumor growth [18]. According to related studies, there are a few mRNAs that can regulate tumor angiogenesis. For example, miR-145 inhibits angiogenesis in osteosarcoma. The underlying mechanism may be related to its inhibition of VEGF expression; however, no studies have explored this finding in detail [19].

In the present study, we demonstrated that miR-145 expression levels in MDA-MB-231 cells were lower than those in healthy breast cells, which is consistent with previous reports. Wang et al. [20] and Shayestehpour et al. [21] found that miR-145 was expressed at low levels in esophageal cancer and prostate cancer. Tang et al. [22] reported that the downregulation of miR-145 in osteosarcoma was probably related to osteosarcoma aggressiveness and metastasis, and it may serve as an independent prognosis indicator for patients with osteosarcoma. We transfected MDA-MB-231 cells with an miR-145 overexpression vector. As a result, miR-145 expression levels in miR-145-mimics increased significantly, suggesting that the transfection was successful. The study further indicated that the radiosensitivity of MDA-MB-231 cells increased after miR-145 was overexpressed. According to Gong et al. [23], miR-145 expression reduced the chemoradiation resistance of glioblastoma and inhibited proliferation, migration, and invasion in prostate cancer cells, indicating that miR-145 can also modulate radiosensitivity.

Nevertheless, the underlying mechanism of miR-145 in breast cancer radiotherapy remains unclear. Our study found that OCT4 mRNA and protein levels in miR-145-mimics were decreased. We also verified that miR-145 is capable of binding to the 3 UTR region of OCT4. Yan et al. [24] found that miR-145 increased the radiosensitivity of cervical cancer cells by inactivating OCT4, which further supports our find-

ings. We also found that E-cadherin protein levels were increased, whereas vimentin protein levels were reduced as a result of the miR-145-mimics. This indicates that upregulated miR-145 expression can inhibit EMT in MDA-MB-231 cells and suggests that miR-145 is relevant to EMT in regulating cell proliferation and apoptosis. Steinestel et al. [25] indicated that the contribution of the EMT process to tumor cell invasion and metastasis was related to the loss of E-cadherin expression. Furthermore, they concluded that the EMT-like cell phenotype was associated with increased drug resistance to conventional treatments such as chemotherapy, radiation therapy, or hormone withdrawal.

We also found that the OCT4 mRNA and protein level, after co-transfection of OCT4 and miR-145 overexpression, was higher than that of miR-145 overexpression alone. In contrast, the E-cadherin protein level and apoptosis were decreased, whereas vimentin and cell proliferation increased. The SF of group A was dramatically lower than that of group B. These findings indicate that the tumor suppressive mechanism of miR-145 lies in its ability to target OCT4, which is in line with the findings of Ling et al. [26].

In summary, miR-145 expression was reduced in BCCs and miR-145 overexpression induced EMT. This resulted in the modulation of cell proliferation, relocation, and increased radiosensitivity, which may be related to the specific binding sites within the 3 UTR of OCT4.

Disclosure of conflict of interest

None.

Address correspondence to: Lingling Ye, Galactophore Department of The Second Affiliated Hospital, Guangzhou University of Chinese Medicine, No.55, Inner Ring West Road, University Town, Panyu District, Guangzhou 510000, Guangdong Province, China. Tel: +86-0757-23375538/+86-15626217616; E-mail: ylllcj@163.com

References

[1] Singh SK, Singh S, Lillard JW Jr and Singh R. Drug delivery approaches for breast cancer. Int J Nanomedicine 2017; 12: 6205-6218.

[2] Quan Y, Huang X and Quan X. Expression of miRNA-206 and miRNA-145 in breast cancer and correlation with prognosis. Oncol Lett 2018; 16: 6638-6642.

[3] Coles CE, Griffin CL, Kirby AM, Titley J, Agrawal RK, Alhasso A, Bhattacharya IS, Brunt AM, Ciurlionis L, Chan C, Donovan EM, Emson MA, Harnett AN, Haviland JS, Hopwood P, Jefford ML, Kaggwa R, Sawyer EJ, Syndikus I, Tsang YM, Wheatley DA, Wilcox M, Yarnold JR and Bliss JM. Partial-breast radiotherapy after breast conservation surgery for patients with early breast cancer (UK IMPORT LOW trial): 5-year results from a multicentre, randomised, controlled, phase 3, non-inferiority trial. Lancet 2017; 390: 1048-1060.

[4] Taylor C, Correa C, Duane FK, Aznar MC, Anderson SJ, Bergh J, Dodwell D, Ewertz M, Gray R, Jagsi R, Pierce L, Pritchard KI, Swain S, Wang Z, Wang Y, Whelan T, Peto R and McGale P. Estimating the risks of breast cancer radiotherapy: evidence from modern radiation doses to the lungs and heart and from previous randomized trials. J Clin Oncol 2017; 35: 1641-1649.

[5] Azimian H, Dayyani M, Toossi MTB and Mahmoudi M. Bax/Bcl-2 expression ratio in prediction of response to breast cancer radiotherapy. Iran J Basic Med Sci 2018; 21: 325-332.

[6] Li B, Zhu X, Ward CM, Starlard-Davenport A, Takezaki M, Berry A, Ward A, Wilder C, Neunert C, Kutlar A and Pace BS. MIR-144-mediated NRF2 gene silencing inhibits fetal hemoglobin expression in sickle cell disease. Exp Hematol 2019; 70: 85-96.e85.

[7] Wang J, Chen J and Sen S. MicroRNA as biomarkers and diagnostics. J Cell Physiol 2016; 231: 25-30.

[8] El Bezawy R, Tinelli S, Tortoreto M, Doldi V, Zuco V, Folini M, Stucchi C, Rancati T, Valdagni R, Gandellini P and Zaffaroni N. miR-205 enhances radiation sensitivity of prostate cancer cells by impairing DNA damage repair through PKCε and ZEB1 inhibition. J Exp Clin Cancer Res 2019; 38: 51.

[9] Huang X, Yuan T, Liang M, Du M, Xia S, Dittmar R, Wang D, See W, Costello BA, Quevedo F, Tan W, Nandy D, Bevan GH, Longenbach S, Sun Z, Lu Y, Wang T, Thibodeau SN, Boardman L, Kohli M and Wang L. Exosomal miR-1290 and miR-375 as prognostic markers in castration-resistant prostate cancer. Eur Urol 2015; 67: 33-41.

[10] Zargar H, Espiritu PN, Fairey AS, Mertens LS, Dinney CP, Mir MC, Krabbe LM, Cookson MS, Jacobsen NE, Gandhi NM, Griffin J, Montgomery JS, Vasdev N, Yu EY, Youssef D, Xylinas E, Campain NJ, Kassouf W, Dall'Era MA, Seah JA, Ercole CE, Horenblas S, Sridhar SS, McGrath JS, Aning J, Shariat SF, Wright JL, Thorpe AC, Morgan TM, Holzbeierlein JM, Bivalacqua TJ,

North S, Barocas DA, Lotan Y, Garcia JA, Stephenson AJ, Shah JB, van Rhijn BW, Daneshmand S, Spiess PE and Black PC. Multicenter assessment of neoadjuvant chemotherapy for muscle-invasive bladder cancer. Eur Urol 2015; 67: 241-249.

[11] Ding Y, Zhang C, Zhang J, Zhang N, Li T, Fang J, Zhang Y, Zuo F, Tao Z, Tang S, Zhu W, Chen H and Sun X. miR-145 inhibits proliferation and migration of breast cancer cells by directly or indirectly regulating TGF-β1 expression. Int J Oncol 2017; 50: 1701-1710.

[12] Wang X, Wang E, Cao J, Xiong F, Yang Y and Liu H. MiR-145 inhibits the epithelial-to-mesenchymal transition via targeting ADAM19 in human glioblastoma. Oncotarget 2017; 8: 92545-92554.

[13] Ye D, Shen Z and Zhou S. Function of microRNA-145 and mechanisms underlying its role in malignant tumor diagnosis and treatment. Cancer Manag Res 2019; 11: 969-979.

[14] Ye P, Shi Y, An N, Zhou Q, Guo J and Long X. miR-145 overexpression triggers alteration of the whole transcriptome and inhibits breast cancer development. Biomed Pharmacother 2018; 100: 72-82.

[15] Hu J, Qiu M, Jiang F, Zhang S, Yang X, Wang J, Xu L and Yin R. MiR-145 regulates cancer stem-like properties and epithelial-to-mesenchymal transition in lung adenocarcinoma-initiating cells. Tumour Biol 2014; 35: 8953-8961.

[16] Han Q, Zhang HY, Zhong BL, Wang XJ, Zhang B and Chen H. MicroRNA-145 inhibits cell migration and invasion and regulates epithelial-mesenchymal transition (EMT) by targeting connective tissue growth factor (CTGF) in esophageal squamous cell carcinoma. Med Sci Monit 2016; 22: 3925-3934.

[17] Lamouille S, Xu J and Derynck R. Molecular mechanisms of epithelial-mesenchymal transition. Nat Rev Mol Cell Biol 2014; 15: 178-196.

[18] Kong W, He L, Richards EJ, Challa S, Xu CX, Permuth-Wey J, Lancaster JM, Coppola D, Sellers TA, Djeu JY and Cheng JQ. Upregulation of miRNA-155 promotes tumour angiogenesis by targeting VHL and is associated with poor prognosis and triple-negative breast cancer. Oncogene 2014; 33: 679-689.

[19] Lei P, Xie J, Wang L, Yang X, Dai Z and Hu Y. microRNA-145 inhibits osteosarcoma cell proliferation and invasion by targeting ROCK1. Mol Med Rep 2014; 10: 155-160.

[20] Wang XC, Zhang ZB, Wang YY, Wu HY, Li DG, Meng AM and Fan FY. Increased miRNA-22 expression sensitizes esophageal squamous cell carcinoma to irradiation. J Radiat Res 2013; 54: 401-408.

[21] Shayestehpour M, Moghim S, Salimi V, Jalilvand S, Yavarian J, Romani B, Ylösmäki E and Mokhtari-Azad T. Selective replication of miR-145-regulated oncolytic adenovirus in MCF-7 breast cancer cells. Future Virol 2016; 11: 671-680.

[22] Tang M, Lin L, Cai H, Tang J and Zhou Z. MicroRNA-145 downregulation associates with advanced tumor progression and poor prognosis in patients suffering osteosarcoma. Onco Targets Ther 2013; 6: 833-838.

[23] Gong P, Zhang T, He D and Hsieh JT. MicroRNA-145 modulates tumor sensitivity to radiation in prostate cancer. Radiat Res 2015; 184: 630-638.

[24] Yan S, Li X, Jin Q and Yuan J. MicroRNA-145 sensitizes cervical cancer cells to low-dose irradiation by downregulating OCT4 expression. Exp Ther Med 2016; 12: 3130-3136.

[25] Steinestel K, Eder S, Schrader AJ and Steinestel J. Clinical significance of epithelial-mesenchymal transition. Clin Transl Med 2014; 3: 17.

[26] Ling DJ, Chen ZS, Zhang YD, Liao QD, Feng JX, Zhang XY and Shi TS. MicroRNA-145 inhibits lung cancer cell metastasis. Mol Med Rep 2015; 11: 3108-3114.